

**A TWO-CHANNEL PHOSWICH DETECTOR FOR DUAL AND TRIPLE COINCIDENCE
MEASUREMENTS OF RADIOXENON ISOTOPES**

Abi T. Farsoni, David M. Hamby, Kimberly D. Ropon, and Sean E. Jones

Oregon State University

Sponsored by National Nuclear Security Administration
Office of Nonproliferation Research and Development
Office of Defense Nuclear Nonproliferation

Contract No. DE-FC52-06NA27322

ABSTRACT

As part of the Comprehensive Nuclear Test Ban Treaty, the International Monitoring System (IMS) has been established for monitoring xenon radioisotopes in the atmosphere to detect atmospheric or underground nuclear explosions. Experimental results from the Automated Radioxenon Sampler/Analyzer (ARSA) system, developed at Pacific Northwest National Laboratory, show that the system is capable of detecting very low concentrations of the fission product radioxenon isotopes ^{133}Xe , $^{133\text{m}}\text{Xe}$, $^{131\text{m}}\text{Xe}$ and ^{135}Xe . To build a more practical radioxenon detection system as sensitive as the ARSA system but with reduced cost, size, power consumption and complexity, several detection systems have been developed or are currently under development.

It has been shown (McIntyre et al. 2004) that triple coincidence measurements of beta, conversion electrons (CE) and x-ray from the radioxenon gas provides a significant reduction of Compton scatter interference in the 30-keV line and therefore much lower (2–3 orders of magnitude) concentrations of ^{133}Xe can be detected even with a high radon background. The triple coincidence measurement eliminates the need for additional separation columns and traps (required for removing the background radon) and allows for reduced passive shielding as well, thus reducing the size and power consumption of the system.

In this paper, a two-channel phoswich detector is introduced and studied. The detector consists of a thin hollow disk (with 2 mm thickness and 76.2 mm diameter) as the xenon gas cell, surrounded by two identical planar triple-layer phoswich detectors. This design provides a solid angle of about 3.4π for the gas cell, close to that of the ARSA system ($\sim 3.5\pi$). The planar shape of the detectors has several important advantages, among which are the reduced cost due to its simplicity, and because it has a minimum non-uniformity in light collection efficiency, will not unreasonably degrade the beta or gamma energy resolution. Moreover, utilizing digital signal processing for the proposed two-channel beta/gamma detection system, gamma-ray singles, beta singles, (β/γ) coincidence and $(\beta/\text{CE}/\text{x-ray})$ triple coincidence signals can be detected. Monte Carlo modeling of radiation transport and light collection were performed to study the phoswich detector response, and will be discussed in this paper.

Report Documentation Page				Form Approved OMB No. 0704-0188	
Public reporting burden for the collection of information is estimated to average 1 hour per response, including the time for reviewing instructions, searching existing data sources, gathering and maintaining the data needed, and completing and reviewing the collection of information. Send comments regarding this burden estimate or any other aspect of this collection of information, including suggestions for reducing this burden, to Washington Headquarters Services, Directorate for Information Operations and Reports, 1215 Jefferson Davis Highway, Suite 1204, Arlington VA 22202-4302. Respondents should be aware that notwithstanding any other provision of law, no person shall be subject to a penalty for failing to comply with a collection of information if it does not display a currently valid OMB control number.					
1. REPORT DATE SEP 2007		2. REPORT TYPE		3. DATES COVERED 00-00-2007 to 00-00-2007	
4. TITLE AND SUBTITLE A Two-Channel Phoswich Detector for Dual and Triple Coincidence Measurements of Radioxenon Isotopes				5a. CONTRACT NUMBER	
				5b. GRANT NUMBER	
				5c. PROGRAM ELEMENT NUMBER	
6. AUTHOR(S)				5d. PROJECT NUMBER	
				5e. TASK NUMBER	
				5f. WORK UNIT NUMBER	
7. PERFORMING ORGANIZATION NAME(S) AND ADDRESS(ES) Oregon State University, Corvallis, OR, 97331-4501				8. PERFORMING ORGANIZATION REPORT NUMBER	
9. SPONSORING/MONITORING AGENCY NAME(S) AND ADDRESS(ES)				10. SPONSOR/MONITOR'S ACRONYM(S)	
				11. SPONSOR/MONITOR'S REPORT NUMBER(S)	
12. DISTRIBUTION/AVAILABILITY STATEMENT Approved for public release; distribution unlimited					
13. SUPPLEMENTARY NOTES Proceedings of the 29th Monitoring Research Review: Ground-Based Nuclear Explosion Monitoring Technologies, 25-27 Sep 2007, Denver, CO sponsored by the National Nuclear Security Administration (NNSA) and the Air Force Research Laboratory (AFRL)					
14. ABSTRACT see report					
15. SUBJECT TERMS					
16. SECURITY CLASSIFICATION OF:			17. LIMITATION OF ABSTRACT Same as Report (SAR)	18. NUMBER OF PAGES 10	19a. NAME OF RESPONSIBLE PERSON
a. REPORT unclassified	b. ABSTRACT unclassified	c. THIS PAGE unclassified			

OBJECTIVE

Several prototypic radioxenon detection systems have been developed to monitor atmospheric or underground nuclear explosions by measuring the concentration of the four xenon radioisotopes: $^{131\text{m}}\text{Xe}$, $^{133\text{m}}\text{Xe}$, $^{135\text{g}}\text{Xe}$, and $^{135\text{m}}\text{Xe}$. To increase the sensitivity, these systems detect radioxenons via a beta-gamma coincidence counting. The ARSA system developed at the Pacific Northwest National Laboratory is one such system which is generally considered as a reference system since its sensitivity to detect ultra-low concentrations of radioxenons has been proven in several field tests (McIntyre et al. 2006). The ARSA system has four plastic (BC-404) gas cells, each coupled to a pair of PMTs, to hold the xenon gas and detect beta/CE particles as well. Gamma- and x-rays are detected by two optically isolated NaI(Tl) crystals, each viewed by two PMTs (McIntyre et al., 2001).

Despite its sensitivity, the ARSA system needs very careful gain matching and calibration, which is not always easy to achieve. Memory effect and radon interference are among other issues which the ARSA system faces. Previous tests of the ARSA system have shown that latent radioxenon and radon remains in the gas cells even after evacuation of the gases, leading to a memory effect which increases the background level for subsequent measurements. The current technology for separating ambient xenon from the air is also very efficient at collecting ambient radon. Additional separation columns and traps are required to remove the radon and consequently increase system size and power consumption.

Employing the phoswich technology with a beta-gamma coincidence counting capability accompanied by digital signal processing of PMT pulses can simplify radioxenon detection. In a phoswich detector, two or more scintillation layers are coupled to a single PMT. The energy deposition in each layer from incident beta and/or gamma, in coincidence or singles, are then determined via digital pulse shape analysis of the PMT's anode pulses (Ely et al., 2003; Hennig et al., 2006; and Farsoni and Hamby, 2007).

To enhance radioxenon detection, based on previous work (Farsoni and Hamby, 2006) and considering manufacturing limitations, a two-channel phoswich detector has been designed, modeled, and ordered. The detector consists of a thin hollow disk (2 mm thickness and 76.2 mm diameter) as the xenon gas cell, surrounded by two identical planar triple-layer phoswich detectors. In designing the detector, several priorities have been considered, including reducing the memory effect; improving the 30 keV x-ray/(CE + beta) coincidence region; increasing the system sensitivity by employing both dual and triple coincidence counting; improving light collecting uniformity; and decreasing the overall cost through simplifying the detector design. A two-channel digital pulse processor is under development and will be employed to detect and digitally process coincidence signal pulses.

RESEARCH ACCOMPLISHED

Two-Channel Phoswich Detector

Various geometries and phoswich designs were investigated to meet both the radioxenon detection requirements and current available manufacturing capabilities. Choosing the shape of the gas cell was the most important part of this study. To enhance the beta/CE detection and minimize the partial energy absorption in xenon gas itself, the average travel distance from the source to the beta layer must be minimized. Also, to reduce cost, the shape of the gas cell should be as simple as possible. In particular for multi-layer scintillation detectors, any irregular shape will increase the overall cost, and because of non-uniformity in light collection efficiency, irregularities degrade system energy resolution. Therefore, the simplest design was chosen: a thin hollow disk, 2-mm thick and 76.2-mm in diameter, which accommodates 9.12 cm³ of sample gas (the ARSA's gas cell has a volume of 6.14 cm³). The gas cell is surrounded by two identical planar phoswich detectors. An aluminum sleeve is used to join the two detectors and completes the gas cell. This design provides a solid angle of about 3.4π for the gas cell, close to that of the ARSA system ($\sim 3.5 \pi$).

Compared with a single-channel phoswich detector (i.e., phoswich well-type detector, Hennig et al., 2006), which is able to detect only dual coincidences (β/γ and $(CE + \beta)/x\text{-ray}$), the proposed two-channel design is able to work in both dual and triple coincidence modes. Besides dual coincidences, ^{133}Xe and ^{135}Xe have a triple coincidence ($\beta/CE/x\text{-ray}$). The triple coincidence provides further reduction in the Compton background and the interference from radon daughters in a two-dimensional beta/gamma coincidence energy distribution (McIntyre et al., 2004). This eliminates the need for additional separation columns and traps (required for removing the background radon) and allows for reduced passive shielding as well, thus reducing system size and power consumption.

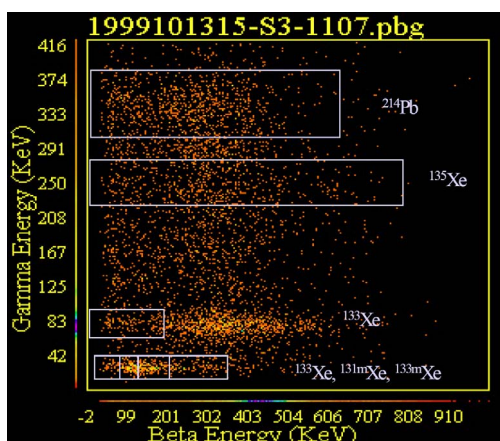


Figure 1. Two-dimensional beta/gamma spectrum (taken from McIntyre et al., 2006).

Generally, a two-dimensional beta/gamma spectrum is used to monitor xenon radioisotopes in the ARSA system (Figure 1). There are three boxed areas (in the absence of any radon daughters) from which the concentration of four radioxenons can be calculated. These areas are located at three gamma/x-ray energies; 30, 80, and 250 keV. The 30 keV x-ray area is the most complicated and needs more attention since it contains energy depositions from three xenon radioisotopes: ^{133}Xe , which emits beta (E_{max} 346 keV) and CE (45 keV); $^{131\text{m}}\text{Xe}$, which emits CE (129 keV); and $^{133\text{m}}\text{Xe}$, which emits CE (199 keV). As seen in Figure 1, and shown in more detail in Figure 2, this area is divided into three regions; Region I, II, and III for detecting $^{131\text{m}}\text{Xe}$, $^{133\text{m}}\text{Xe}$, and ^{133}Xe , respectively. Region III has two parts, the left and right extremes, of which their sum is used for ^{133}Xe concentration calculations (McIntyre et al., 2006).

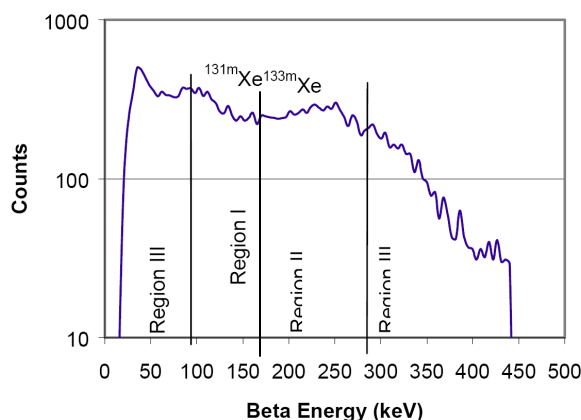


Figure 2. The 30 keV gamma-gated beta-spectrum for pure ^{133}Xe divided into three regions to discriminate two metastable radioxenons, $^{131\text{m}}\text{Xe}$ and $^{133\text{m}}\text{Xe}$ (taken from McIntyre et al., 2006).

The minimum detectable concentration (MDC) of ^{131m}Xe and ^{133m}Xe can be improved if the background in the corresponding regions (I and II) is reduced. There are two main sources of “background” in these regions in a dual coincidence counter: Compton scatter from gamma-rays with higher energies and beta particles from ^{133}Xe (E_{max} 346 keV). Employing the two-channel phoswich detector and a triple coincidence measurement, we introduce a new pulse processing method where the background under these regions due to ^{133}Xe can be reduced approximately by half (Figure 3). From this Figure, the eight possible triple-coincidence scenarios can be divided into two scenario groups: one group where the beta particle and conversion electron are detected in the same phoswich and the other group where the beta particle is detected by one phoswich and the conversion electron is detected by the other phoswich. In the first group, beta particles and conversion electrons (45 keV) are absorbed in a single phoswich and cannot be separated, thus the resulting pulse from the beta layer is recorded in the beta spectrum. This situation can be observed in the two-dimensional spectrum from the ARSA system as well (Figure 1), due to simultaneous absorption of conversion electrons and betas; the 30 keV-gated beta spectrum is shifted to higher energies, i.e., summed with CE, 45 keV. In the second group (scenarios 5 to 8), the beta particle and conversion electron are absorbed in opposite phoswich detectors; thus, they can be separated when a triple event is identified and confirmed by detecting a 30 keV x-ray in one of two phoswich detectors. Now, without losing any useful information, the beta event can be rejected while the CE event is recorded in the beta spectrum, resulting in reduction of the beta-background in Regions I and II. In fact, by using this technique, 50% of the triple-coincidence events previously recorded in Regions I, II, and III (right) from ^{133}Xe are now shifted and recorded in Region III (left), significantly improving in the MDC of ^{131m}Xe and ^{133m}Xe . In the ARSA system, only dual coincidence events in the 80 keV and some events in the 30 keV areas (Region III, left and right) are used for calculating the ^{133}Xe concentration. The MDC of ^{133}Xe itself, therefore, can be improved by this technique as well, since Region III (left) now contains some triple coincidence events which previously were lost in Regions I and II.

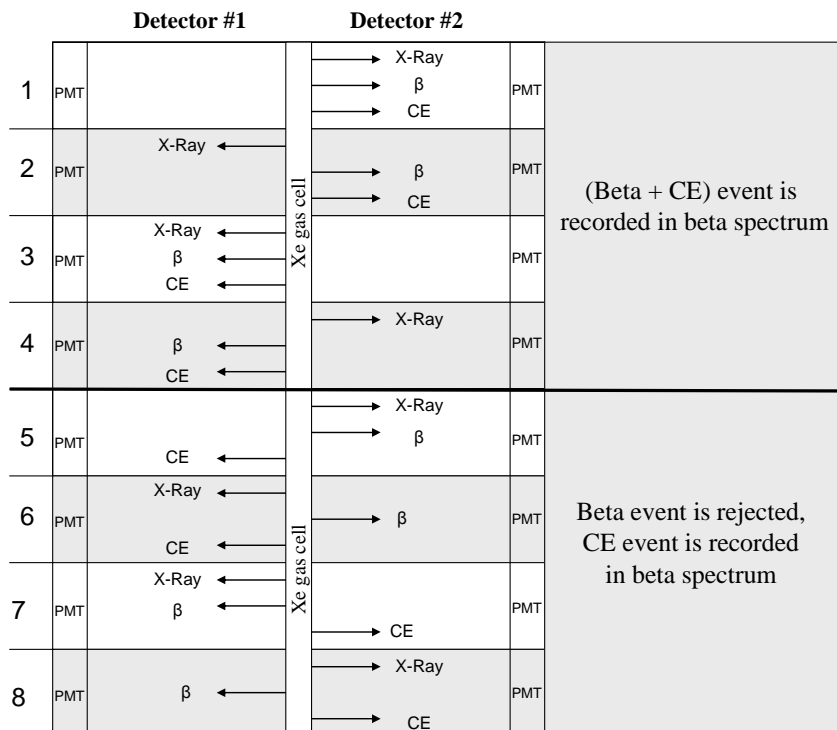


Figure 3. Employing two different pulse processing schemes for eight possible scenarios when a triple coincidence event in 30 keV x-ray area is detected.

Triple-Layer Phoswich Design

In the simplest design for a beta/gamma planar phoswich detector, two scintillation layers with sufficiently different decay times are used. Generally, the first layer from low-Z materials is intended for beta spectroscopy while the second layer from high-Z materials is assigned for gamma detection. A plastic scintillator might be the best choice for beta detection since it can be easily built in very thin layers, minimizes backscatter, and creates minimal bremsstrahlung radiation. Since most plastic scintillators possess very fast decay times (a few nsec), to facilitate the digital pulse-shape processing, a relatively slow and high-Z scintillator should be selected for gamma-ray detection. Among the inorganics, two scintillators are the most attractive ones: CsI(Tl) and NaI(Tl). Unfortunately both of these scintillators are hygroscopic and should be isolated from the plastic scintillator by a quartz optical window. The minimum quartz window offered by our detector manufacturer (Saint Gobain Crystals & Detectors), was 6.35 mm which was not acceptable for detecting 30 keV x-rays (see the simulated photon efficiency of NaI(Tl)* in Figure 5). Our MCNP simulations, however, show that adding a 2-mm CaF_2 layer between the plastic scintillator (1.5 mm of BC-400) and the quartz optical window will improve the detection efficiency of 30 keV x-rays by a factor of about 7, but will reduce the efficiency of 81 and 250 keV gamma-rays by 5% and 2%, respectively. Therefore, since the 30 keV x-ray regions carry vital spectral information for detecting the three radionuclides, it was decided to design the phoswich detector with three scintillation layers: BC-400 (2.4 nsec) for beta particle and CE detection, CaF_2 (900 nsec) for 30 keV x-ray detection and NaI (230 nsec) for gamma-ray detection.

Figure 4 shows the two-channel triple-layer phoswich detector design. The thickness of BC-400 is 1.5 mm and is sufficient to absorb most of the beta/CE particles emitted from radionuclides. The thicknesses of the CaF_2 and NaI(Tl) layers were chosen to be 2.0 and 25.4 mm, respectively.

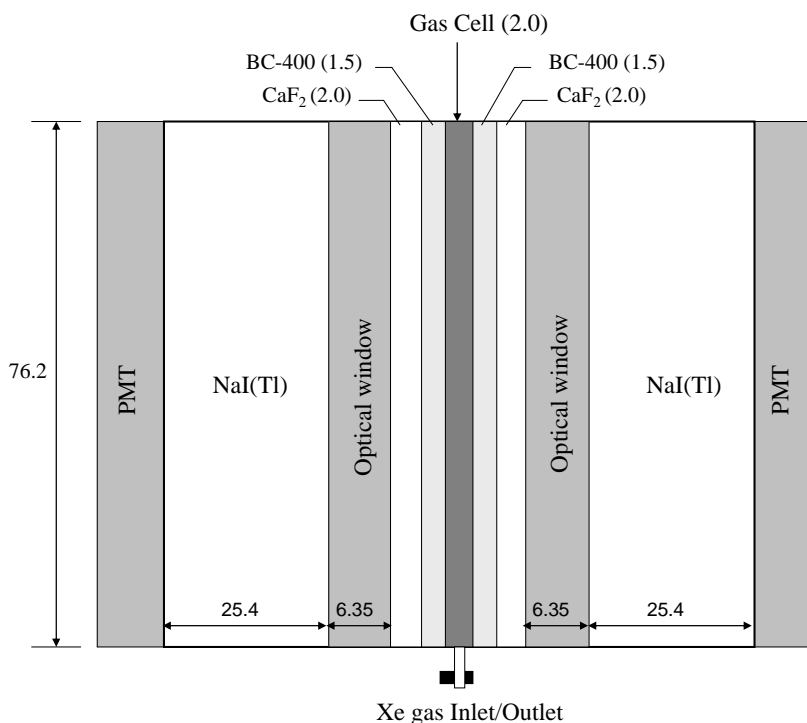


Figure 4. Schematic arrangement of the two-channel phoswich detector. All dimensions are in mm.

MCNP Analysis

A Monte Carlo analysis using the MCNP5 code was performed to study the response of the triple-layer phoswich detector to incident beta/CE and gamma/x-rays from xenon radioisotopes. Except for the simulations presented in Figure 9, for simplicity all simulations were performed in a single detector. Also in all simulations, the gas sample was a mixture of xenon and helium gas, a 10-keV threshold was applied for all simulated results and a very thin layer of aluminum (1 μm) was assumed to exist (deposited) on the surface of the BC-400 (facing the gas cell). Use of a 1- μm aluminum layer on plastic scintillators has clearly demonstrated a reduced memory effect from radionuclides remaining in the cells after evacuation (Seifert, 2005). Additionally, this layer will optically isolate the two halves of the detection system.

The simulated total interaction probability as a function of photon energy in sample gas, BC-400, CaF_2 and NaI(Tl) of the triple-layer phoswich detector is shown in Figure 5a. To investigate the effectiveness of using 2-mm CaF_2 for detecting low-energy photons, the simulation (indicated by NaI(Tl)^*) was also executed for a dual-layer phoswich version consisting of BC-400/quartz optical window/ NaI(Tl) with the same thicknesses as used in previous simulations. As expected, in the dual-layer version, only a small fraction ($\sim 5\%$) of 30 keV photons reach and interact with the NaI(Tl)^* layer due to the quartz optical window. In the triple-layer version, however, the 30 keV photons can be detected in the CaF_2 with a significantly increased efficiency of about 36% (a total efficiency of 72% for both sides of the detector). With an increase in the photon energy, the CaF_2 efficiency decreases rapidly and the efficiency of both the NaI(Tl) and NaI(Tl)^* increases. The detection efficiencies for 81 and 250 keV photons in NaI(Tl)^* are 27% and 25%, and are 22% and 24% respectively for NaI(Tl) . The photoelectric efficiencies of the CaF_2 and NaI(Tl) for photons of different energies are depicted in Figure 5b. Although possessing a lower Z , the CaF_2 shows a photoelectric fraction (photoelectric/total probability ratio) of about 99% for 30 keV photons.

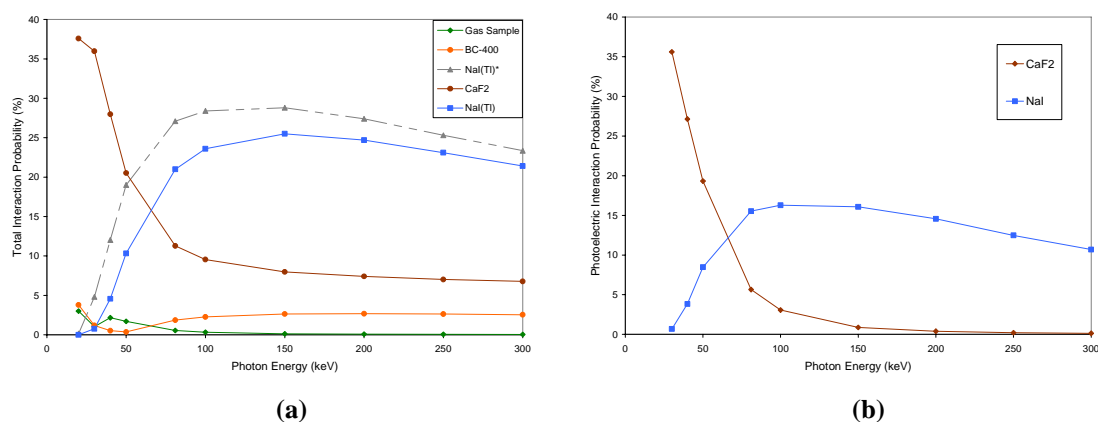


Figure 5. (a) Total interaction probability of photons with xenon gas, BC-400, CaF_2 and NaI(Tl) in the triple-layer phoswich detector (NaI(Tl)^* is from the 2-layer version and is given for reference, see the text) and (b) photoelectric interaction probability of photons with CaF_2 and NaI(Tl) . The figure shows the simulations for one side of the detection system.

By re-executing the photon simulation for different thicknesses of the CaF_2 layer, changes in detection efficiency of the CaF_2 and NaI(Tl) were examined for photon energies of most interest (30, 81, and 250 keV)(Figure 6). We found that a 2.0 mm thickness of CaF_2 was a good choice since its 30 keV efficiency versus thickness follows a non-linear increase, while beyond this thickness it shows an approximate linear function. For the three photon energies, in the range of 1–3 mm of CaF_2 , the detection efficiency of the NaI(Tl) layer decreases linearly, but at different rates.

The simulated interaction probabilities of monoenergetic electrons with layers of the phoswich detector are presented in Figure 7. The BC-400 shows almost a flat efficiency ($\sim 45\%$) for incident electrons with energies higher than about 100 keV. The figure also shows a threshold energy (around 500 keV) for absorption of incident electrons in the CaF_2 ; this is expected since the range of 480 keV electrons in the BC-400 is about 1.5 mm. Although this figure shows a relatively high probability for interacting incident electrons with the gas sample and aluminum window, on average only a very small fraction of electron energy is absorbed in these layers. Simulations show that an average energy of 3.8 keV and 1.8 keV is deposited in the sample gas from incident 50 keV and 900 keV electrons, respectively.

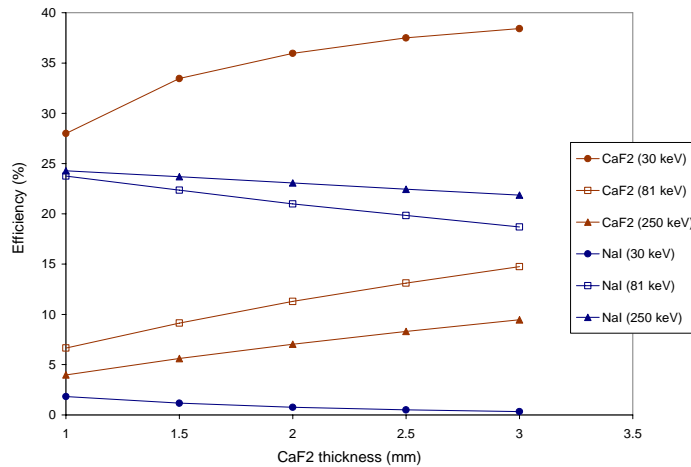


Figure 6. Total efficiencies for the three major photon energies from xenon radioisotopes with CaF_2 and $\text{NaI}(\text{Tl})$, as a function of CaF_2 thickness. For all simulations, the thickness of BC-400 and $\text{NaI}(\text{Tl})$ were 1.5 and 25.4 mm, respectively.

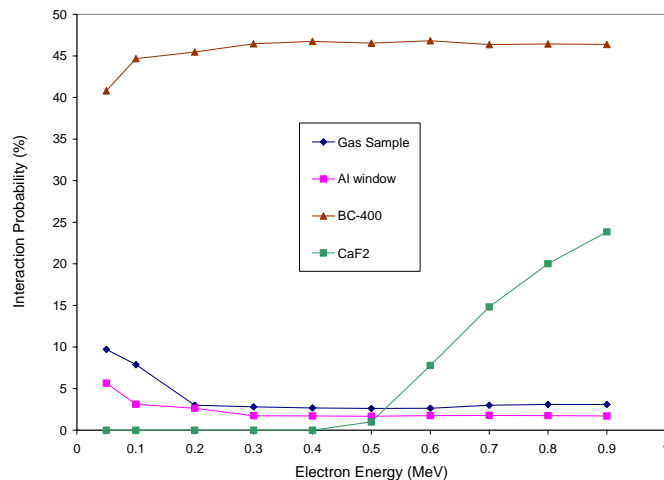


Figure 7. Simulated interaction probabilities as a function of incident electron energy.

The BC-400 layer does not fully stop all beta particles from ^{135}Xe (E_{max} 905 keV) and a small fraction of high energy betas, can penetrate into the CaF_2 layer and produce a false coincidence event. Also, any partial beta energy deposition in intermediate materials (i.e., sample gas and Al window) results in the energy distribution becoming softer. Although this effect is not important for measuring the beta events from ^{135}Xe , it needs more attention for beta particles emitted from ^{133}Xe since it may increase the beta-background in Region I and II (Figure 2; McIntyre, 2006), thus increasing the MDC of $^{131\text{m}}\text{Xe}$ and $^{133\text{m}}\text{Xe}$. To examine these effects, the theoretical beta energy distributions of ^{133}Xe and ^{135}Xe were used to simulate the energy deposition distribution in different layers of the phoswich detector (Figure 8). In Figure 8a, since the BC-400 fully accommodates the highest energy betas (364 keV) from ^{133}Xe , no energy absorption is observed in the CaF_2 layer. For beta particles from ^{135}Xe (Figure 8b), the simulation shows a total efficiency of 1.4% in the CaF_2 layer. For ^{133}Xe , approximately 90% of energy deposition in the sample gas and aluminum window is occurring at energies below 10 keV; this value is 95% for ^{135}Xe . Therefore, by accounting for other effects such as photostatistics and light collection non-uniformity, this level of partial absorption is not expected to add a significant extra beta background to the Regions I and II of the 30 keV x-ray-gated beta spectrum (see Figure 2).

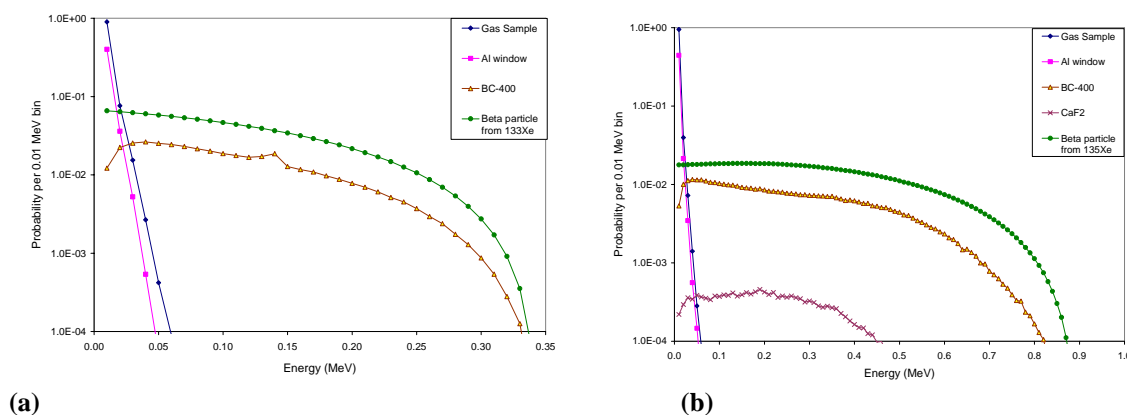


Figure 8. Energy deposition distribution in Xe gas, Al window, BC-400 and CaF_2 from beta particles of (a) ^{133}Xe and (b) ^{135}Xe . Figure also shows the energy distribution of each beta source as reference.

Broadening of the CE peaks (129 and 199 keV), due to partial energy deposition of incident conversion electrons in the plastic scintillator, was studied for both the ARSA and our phoswich detectors. In Figure 9, three gas/beta-cell geometries were studied and compared: the original ARSA gas cell, the ARSA gas cell with interior aluminum coating, and our phoswich gas cell. Energy absorption in the sample gas for the ARSA's gas cell shows a harder distribution than that of the phoswich detector. This results in a higher average energy deposition in the ARSA's gas cell (5.9 keV from 129 keV CE) than in that of the phoswich detector (2.8 keV from 129 keV CE). At both CE energies, the BC-404 layer in the original ARSA system shows a more peaked energy distribution, while the ARSA's gas cell with an aluminum coating shows a broader peak. Therefore, compared with the ARSA system, our first estimate from Figure 9 shows that adding a 1- μm Al coating on the plastic scintillator will not significantly broaden the CE peaks in the x-ray-gated beta spectrum.

Light Collection Efficiency

The uniformity of light collection efficiency in our phoswich design was studied using the Monte Carlo optical simulation software, DETECT2000. In order to produce a continuous and high resolution data set, light was generated in three-hundred individual pixels, covering the entire cross section of the scintillators,

in a plane about the axis of symmetry. One million optical photons of a wavelength attributable to the peak output of its parent scintillator were generated in each pixel, yielding variances on the order of 0.005%. Figure 10-a presents the simulated distribution of light collection efficiency about the detector's line of symmetry, assuming a reflection coefficient of 0.95 on the outer surface of the phoswich detector. To estimate the contribution of non-uniformity of light collection efficiency in the energy resolution, the volume-weighted distribution of light collection efficiency in each scintillation layer of the phoswich detector is calculated and shown in Figure 10b. The peak broadening (resolution) in the volume-weighted distribution of light collection efficiency is about 1.2% and 1.6% for the first two layers and the NaI(Tl), respectively. This small variation in light collection efficiency is a result of the simple and planar shape of the phoswich design and will not add a significant uncertainty to the beta or gamma energy determination.

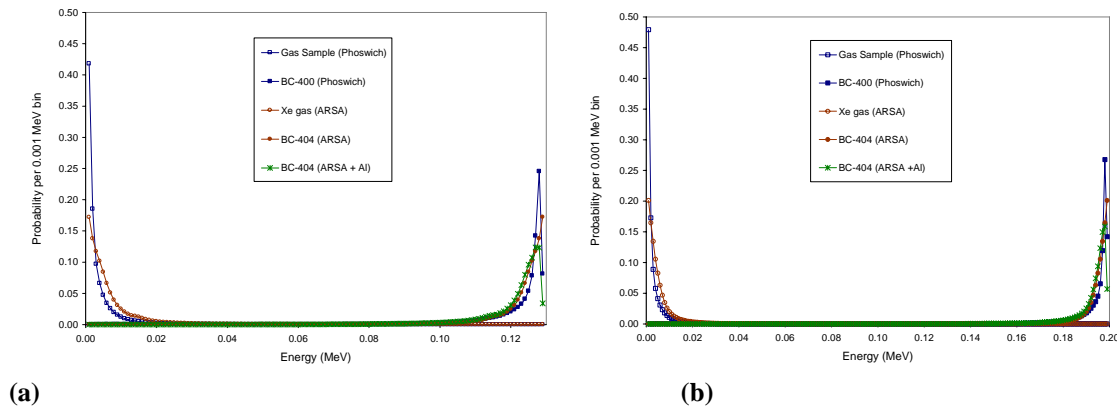


Figure 9. Comparing the response of the ARSA and our phoswich detectors to conversion electrons from (a) ^{131m}Xe (129 keV) and (b) ^{133m}Xe (199 keV).

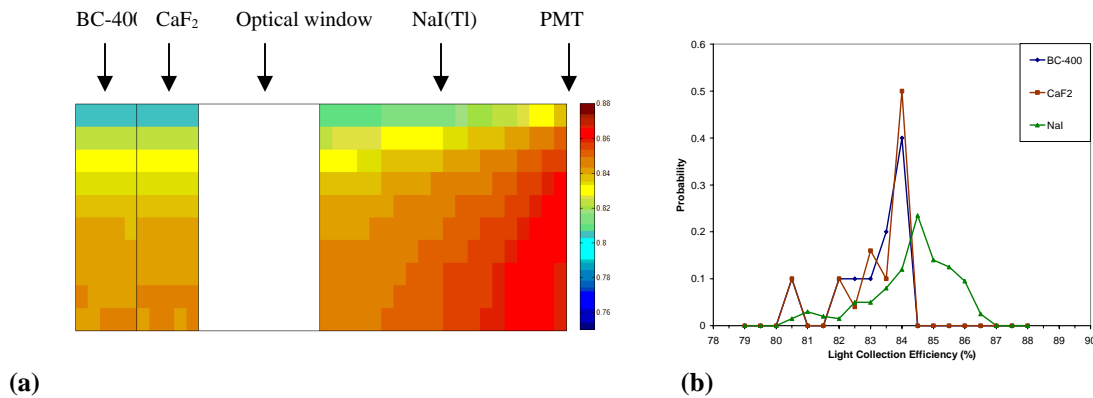


Figure 10. Distribution of light collection efficiency (a) and volume-weighted light collection efficiency (b).

CONCLUSION

To enhance radioxenon detection, a prototypic two-channel phoswich detector has been designed, modeled and ordered. The detector features several advantages over the ARSA system: a reduced memory effect, detection of both dual and triple coincidence events, improved energy resolution due to a minimized non-uniformity in light collection, and a decreased overall cost, size and power consumption. By detecting triple coincidence events, we introduced a new novel technique to significantly improve the MDC of ^{133}Xe , $^{131\text{m}}\text{Xe}$, and $^{133\text{m}}\text{Xe}$. Likewise, the radiation transport modeling presented in this paper shows the advantages of triple-layer over dual-layer phoswich detectors to meet both the requirement for detecting low-energy photons and overcoming manufacturing limitations. As a result of the planar shape of the phoswich design, light collection modeling shows that the phoswich detector has a small non-uniformity in the light collection efficiency and therefore improves energy resolution over other current designs.

REFERENCES

- Ely, J. H., C. E. Aalseth, J. C. Hayes, T. R. Heimbigner, J. I. McIntyre, H. S. Miley, M. E. Panisko, and M. Ripplinger (2003), Novel beta-gamma coincidence measurements using phoswich detectors, in *Proceedings of the 25th Seismic Research Review—Nuclear Explosion Monitoring: Building the Knowledge Base*, LA-UR-03-6029, Vol. 2, pp. 533–541.
- Hennig, W., H. Tan, W. K. Warburton, and J. I. McIntyre (2005). Digital pulse shape analysis with phoswich detectors to simplify coincidence measurements of radioactive xenon, in *Proceedings of the 27th Seismic Research Review: Ground-Based Nuclear Explosion Monitoring Technologies*, LA-UR-05-6407, pp. 787–794.
- Seifert, C. E., J. I. McIntyre, K. C. Antolick, A. J. Carman, M.W. Cooper, J. C. Hayes, T. R. Heimbigner, C. W. Hubbard, K. E. Litke, M. D. Ripplinger, and R. Suarez (2005). Mitigation of memory effects in beta scintillation cells for radioactive gas detection, in *Proceedings of the 27th Seismic Research Review: Ground-Based Nuclear Explosion Monitoring Technologies*, LA-UR-05-6407, pp. 804–814.
- Farsoni, A. T. and D. M. Hamby (2006), Study of a triple-layer phoswich detector for beta and gamma spectroscopy with minimal crosstalk, in *Proceedings of the 28th Seismic Research Review: Ground-Based Nuclear Explosion Monitoring Technologies*, LA-UR-06-5471, pp. 794–792.
- Farsoni, A. T. and D. M. Hamby (2007), A system for simultaneous beta & gamma spectroscopy, *Nuclear Instruments and Methods in Physics Research, Section A* 578: 528–536.
- McIntyre, J. I., K. H. Able, T. W. Bowyer, J. C. Hayes, T. R. Heimbigner, M. E. Panisko, P. L. Reeder, and R. C. Thompson (2001). Measurements of ambient radioxenon levels using the automated radioxenon sampler/analyzer (ARSA), *J. of Radioanalytical and Nuclear Chemistry* 248: 629–635.
- McIntyre, J. I., C. E. Aalseth, T. W. Bowyer, J. C. Hayes, T. R. Heimbigner, S. Morris, and P. L. Reeder (2004). Triple coincidence radioxenon detector, in *Proceedings of the 26th Seismic Research Review: Trends in Nuclear Explosion Monitoring*, LA-UR-04-5801, pp. 581–587.
- McIntyre, J. I., T. W. Bowyer, and P. L. Reeder (2006). Calculation of minimum detectable concentration levels of radioxenon isotopes using the PNLL ARSA system, technical report PNNL-13102.